

Rapid communication

Near-field optics with photonic crystals

S.A. Magnitskii, A.V. Tarasishin, A.M. Zheltikov

International Laser Center, Physics Faculty, Moscow State University, Moscow, 11989, Russia
(Fax: +7-095/939-3113, E-mail: zhelt@ilc.phys.msu.su)

Received: 9 August 1999/Accepted: 18 October 1999/Published online: 10 November 1999

Abstract. Finite-difference time-domain (FDTD) analysis of light propagation in a defect mode of a two-dimensional photonic band-gap (PBG) structure demonstrates that the light field is localized in such a structure within areas with subwavelength ($\lambda/10$) sizes. FDTD simulations reveal efficient formation of an evanescent wave at the output of such a PBG structure, permitting the subwavelength resolution to be achieved in the near field. A probe object with a size less than the wavelength of incident light is shown to perturb the near-field distribution behind the PBG structure and to change the signal detected in the far-field zone. The field intensity distribution inside a PBG structure is also sensitive to the presence of a probe object, offering a way to control the light field localized in defect modes of PBG structures.

PACS: 41.20.Bt; 42.79.-e

Much attention has been recently focused on the investigation of photonic band-gap (PBG) structures [1, 2]. In particular, it was demonstrated that unusual dispersion properties of such structures allow compact tunable optical delay lines to be implemented [3], parameters of short laser pulses to be controlled [4], and nonlinear-optical interactions to be phase-matched [5, 6]. Although the investigation of the field distribution in PBG structures is much more complicated, it opens new fascinating ways to employ photonic crystals. Since no analytical solution can be found to describe the field distribution in this case, such an analysis requires the application of adequate numerical algorithms. Finite-difference time-domain (FDTD) schemes [7] are especially promising for the investigation of PBG structures, as they provide the opportunity to analyze the spatial distribution of the electromagnetic field in PBG structures. The FDTD method has been successfully applied to describe optical switching [8] and pulse compression [4] in nonlinear one-dimensional PBG structures. The FDTD method has also been recently applied for the analysis of the spatial distribution of the electromagnetic field in scanning near-field optical microscopy

(SNOM) [9], allowing important features of signal formation in SNOM systems to be understood. In this paper, we employ the FDTD technique to analyze the propagation of a light beam in a two-dimensional (2D) PBG structure with a defect. This analysis reveals several intriguing features of light localization in such PBG structures, which seem to offer much promise for near-field microscopy. In particular, the localization of light within areas whose sizes are less than a wavelength suggests that a subwavelength resolution can be achieved with PBG structures. We will also demonstrate that the properties of the light field at the output of a 2D PBG structure with a defect are similar to the properties of evanescent waves in near-field optical microscopy, leading us to a concept of PBG components in SNOM.

1 The method of simulations and photonic band-gap structures

In our simulations, we employed the FDTD technique [7], which implies the solution of Maxwell equations with centered finite-difference expressions for space and time derivatives. Keeping in mind that silicon technologies provide an opportunity to fabricate PBG structures in one [6], two [10], and three [11] dimensions, we performed FDTD simulations for macroporous-silicon 2D PBG structures consisting of five to ten periods of cylindrical air holes arranged in a triangular lattice in silicon (Fig. 1) irradiated with a plane light wave coming from $X = -\infty$. The ratio of the hole diameter to the lattice period along the Y axis a was chosen to be equal to 0.95 in order to ensure the maximum width of the band gap for the considered macroporous-silicon structure [12]. The period of the investigated triangular-lattice PBG structure in the X direction was equal to $\sqrt{3}a$. Our FDTD simulations for such a 2D PBG structure without a defect reveal a band gap in the X direction, corresponding to the minimum width of the band gap [12], for a/λ (a is the period of the PBG structure and λ is the wavelength of incident light) ranging from 0.35 to 0.52 for H waves and from 0.44 to 0.57 for E waves, which indicates the existence of a closed band gap and agrees well

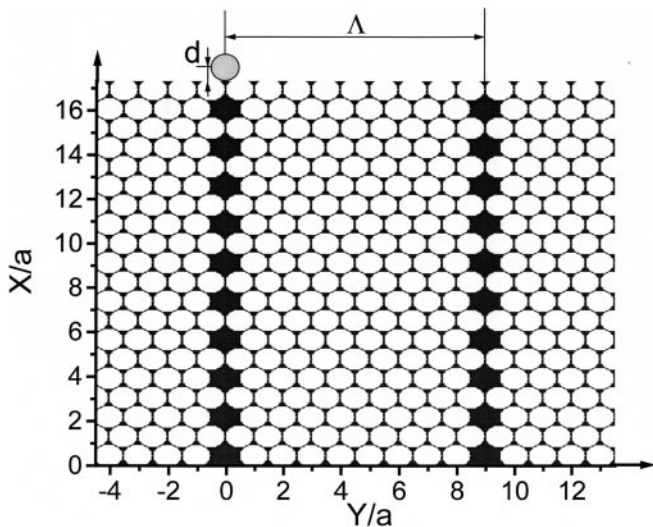


Fig. 1. A fragment of a silicon 2D PBG structure with a defect. A small transparent probe sphere with a refractive index of 1.5 is placed adjacent to the output plane of the PBG structure, with the center of this sphere at a distance d from the output plane of the PBG structure, disturbing the field intensity distribution inside and outside the PBG structure

with the results of simulations carried out by Meade *et al.* [12] and the experimental and theoretical data presented by Gruening *et al.* [10], thus showing the adequacy of the implemented algorithm.

A defect was introduced into the 2D PBG structure considered above by removing one of the rows of air cylinders periodically (with a period Λ) along the Y axis (Fig. 1), which allowed us to use periodic boundary conditions along the Y axis with a period Λ . In order to suppress reflections from artificial boundaries, we employed standard absorbing boundary conditions [13] while simulating light propagation along the X axis by assuming that absorbing surfaces are located at $X = -5a$ and $X = 23a$. Analysis of a 2D PBG structure with a defect allows us to appreciate several advantages of the FDTD technique. One of them is that FDTD simulations are carried out in real space rather than in the Fourier space, so that a defect in a PBG structure results in virtually no computational complications as compared with a PBG structure without a defect. Another advantage of the FDTD approach is that it provides information concerning the spatial distribution of the field inside and behind a PBG structure, allowing us, in particular, to find the throughput of the defect mode, quantitatively characterize the areas of field localization inside the PBG structure, and determine the spatial distribution of the electromagnetic field emerging from the PBG structure.

2 Results and discussion

The FDTD analysis shows that, whereas in a PBG structure without a defect, the field intensity decays on a spatial scale on the order of λ , resulting in a transmission coefficient of the PBG structure of about 10^{-3} , a light beam in a PBG structure with a defect may propagate along a narrow channel. The transmission coefficient for E waves within the range of a/λ ranging from 0.44 to 0.47 in such a structure increases from 10^{-3} up to 0.5, indicating the appearance of a defect level in the band gap. For H waves, the transmission coef-

ficient may be as high as 0.4. In what follows, we present the results of simulations performed for the frequency of the light field corresponding to the defect mode in the band gap. This frequency was chosen for simulations since the transmission of the PBG structure decays dramatically away from this frequency. Generally, the spectra of defect modes in such 2D PBG structures are very complicated, deserving special analysis, which falls beyond the scope of this paper. The two-dimensional distribution of the mean intensity of the electric field calculated for a 10-period PBG structure whose fragment is shown in Fig. 1 with $a/\lambda = 0.454$ is presented in Fig. 2a. The light beam is channeled along the defect in such a structure, and the field is localized at the center of the defect. At certain points, the beam diameter in the channel (measured at half maximum of the field intensity) may be as small as $\lambda/10$ (Fig. 2a), i.e., approximately five times less than the diffraction limit for a light beam focused in air. Note that a similar spatial resolution can be achieved, for example, with a thin single-mode silicon waveguiding slab. However, the

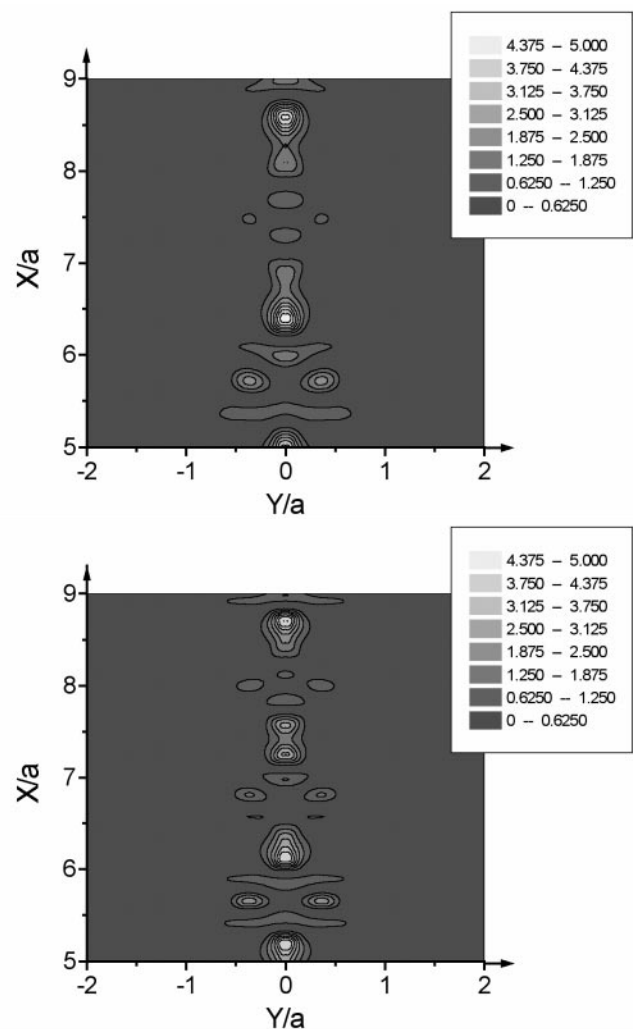


Fig. 2a,b. Two-dimensional map of light localization (field intensity distribution) in a PBG structure whose fragment is shown in Fig. 1: **a** without a probe object and **b** with a $\lambda/4$ probe object whose center is located at the distance $d = \lambda/8$ from the output plane of the PBG structure (see Fig. 1). Gray-scale levels represent the mean values of the electric field squared E^2 for $a/\lambda = 0.454$

way the defect modes are excited in a PBG structure, when no special measures are required to couple radiation into the structure with a sufficiently high efficiency, seems to offer much promise for reducing optical losses and for achieving high-throughput channeling. The light intensity at the center of the defect is several hundred times higher than the intensity at the edges of the channel (Fig. 2a), indicating a high contrast of beam channeling. Channeling of a light beam was observed regardless of the period Λ (for $\Lambda > 2a$), indicating that the effects described above do not result from the interference (cross-talk) of light reflected from neighboring defects. The absence of cross-talk effects in light channeling in such a structure is due to the fact that the penetration depth of light within the band gap is less than the wavelength. The total field intensity behind the crystal over the period Λ along the Y axis remained unchanged, which brings us to a conclusion that the light is channeled only along the defect.

The field intensity distribution behind the PBG structure is presented in Fig. 3a. The field at the output of the PBG structure under these conditions is localized in the transverse direction on a subwavelength spatial scale ($\lambda/10$) and decays exponentially along the X axis. The features of this field are similar to the properties of evanescent waves in SNOM [14], which allows us to propose PBG structures as SNOM components permitting efficient formation of evanescent waves. Since the reciprocity principle is applicable in this case, a PBG structure can be also employed to analyze the evanescent field near a sample, providing an opportunity to implement also the collection mode of SNOM.

Two-dimensional maps in Figs. 3b and 3c show the distribution of the electric field behind the same 2D PBG structure in the case when a small transparent probe sphere with a refractive index of 1.5 and diameters equal $\lambda/4$ (Fig. 3b) and $\lambda/8$ (Fig. 3c) is placed adjacent to the output plane of the PBG structure (as shown in Fig. 1), with the center of this sphere being located at distances $d = \lambda/8$ (Fig. 3b) and $\lambda/16$ (Fig. 3c) from the output plane of the PBG structure. The two-dimensional maps presented in these figures demonstrate that the near-field distribution of the electric field becomes perturbed by a probe object, revealing that the near-field light intensity distribution is highly sensitive to the presence of a probe sphere and suggesting an analogy with the tunneling of the field due to the potential of this sphere.

The integral of the electric-field intensity taken in the $X = 19.7a$ plane also noticeably changes in the presence of the probe sphere. The values of this integral in Figs. 3b,c normalized to the same integral taken in the absence of a probe object (Fig. 3a) are equal to 1.06 and 1.032, respectively, showing that a detector placed in the far-field zone would allow one to easily distinguish between $\lambda/4$ and $\lambda/8$ objects. The integral far-field electric-field intensity calculated with a $\lambda/16$ object placed adjacent to the output plane of the PBG structure was equal to 1.007. Thus, the considered emission-mode scheme of near-field microscopy is characterized by a high sensitivity and a high resolution (see [15, 16]).

The field intensity distribution inside the PBG structure, as can be seen from the comparison of Figs. 2a and 2b, responds to the presence of a probe object by a decrease in the field localization degree. This effect shows the way to control the light field localized in defect modes of PBG structures in various applications of light localization in PBG structures, including nonlinear optics, optical memory, etc.

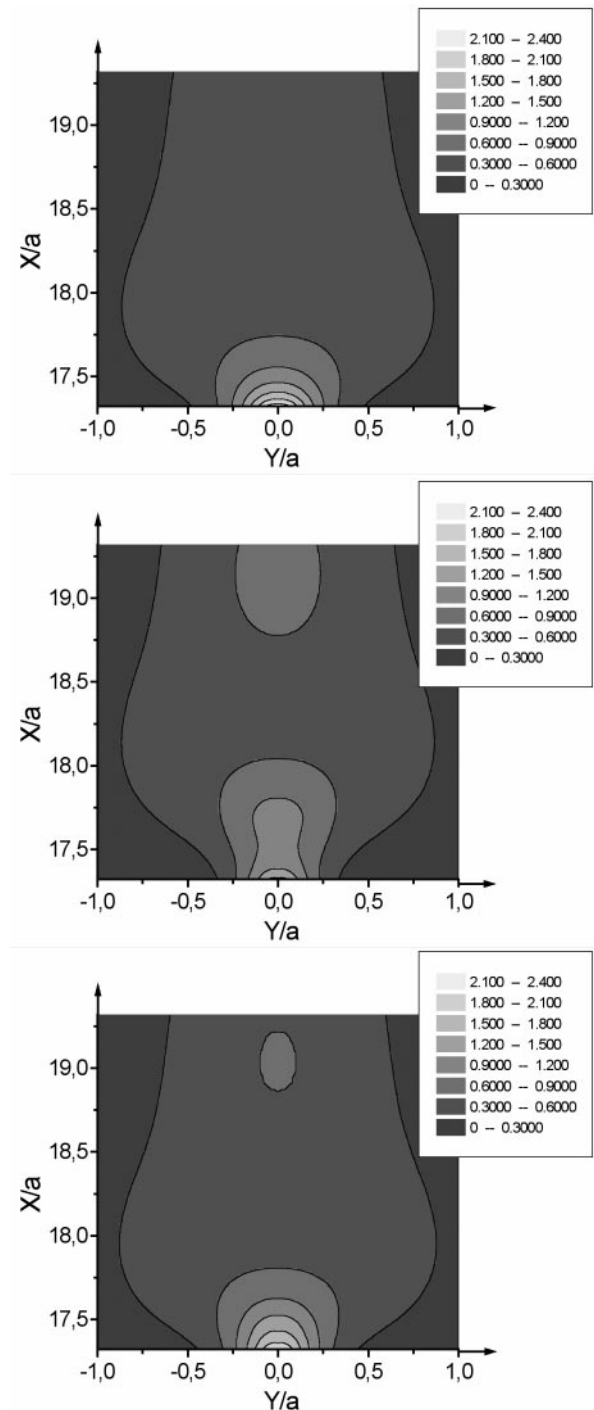


Fig. 3a–c. Two-dimensional map of the field intensity distribution at the output of a 2D PBG structure with a defect whose fragment is shown in Fig. 1: **a** without a probe object and with **b** $\lambda/4$ and **c** $\lambda/8$ probe objects whose centers are located at the distance $d = \lambda/8$ (**b**) and $\lambda/16$ (**c**) from the output plane of the PBG structure (see Fig. 1). Gray-scale levels represent the mean values of the electric field squared E^2 for $a/\lambda = 0.454$

It seems unlikely that some analytical description of the field at the output of the PBG structure considered in this paper could be ever found. However, qualitatively, it is clear that a light beam with a subwavelength diameter produced in a defect mode of a PBG structure cannot freely propagate in air without changing its shape. If the diameter is much less

than the wavelength and contains high-order spatial harmonics, such a beam displays behavior similar to that observed in the evanescent wave, ensuring a subwavelength resolution in the transverse direction in the near field. All the energy of a light beam under these conditions spreads out along the Y coordinate. However, a high concentration of light energy at the output of a 2D PBG structure with a defect can be fully appreciated in the near-field zone. It can be employed, for example, to produce a local excitation, and it can be detected by a tip placed in the near-field zone.

The main advantages of using PBG structures in SNOM are associated with the high resolution that can be achieved because of the high degree of light localization in combination with a high throughput of the defect mode in a PBG structure, ensuring a sufficiently high field strength at the output of a PBG structure. The latter circumstance is associated with the fact that a defect mode of a PBG structure rather than a simple aperture is used to produce an evanescent wave, allowing one to eliminate one of the serious technical difficulties of SNOM, where the throughput of a tip usually drops with the decrease in the aperture size.

Since the energy at the output of a photonic crystal with a defect is high enough, many other applications of evanescent waves produced with a PBG defect mode, apart from those directly related to microscopy proper, can be considered. One of them is creating subwavelength features in photolithography. Another important application could be associated with increasing the density of optical data storage in one, two, and three dimensions. In particular, in three-dimensional optical-memory systems [17], the absence of cross-talk between neighboring defects in the considered PBG structures allows one to implement high-precision addressing for data writing and reading. The field produced at the output of a PBG structure with a defect can be also used to visualize the propagation mode in waveguiding systems, to produce local excitations in samples, and to fabricate subwavelength planar integrated-optics components.

3 Conclusion

FDTD simulations demonstrate that an evanescent field can be efficiently generated with the use of PBG structures, offering a way to achieve subwavelength (on the order of $\lambda/10$) spatial resolution in the scheme of near-field optical microscopy and allowing us to propose PBG structures as com-

ponents of near-field optical microscopy. A probe object with a size less than the wavelength of incident light perturbs the near-field distribution behind the PBG structure as a result of the optical tunneling effect and changes the optical signal detected in the far-field zone. The field intensity distribution inside the PBG structure responds to the presence of a probe object by a decrease in the field localization degree, showing the way to control the light field localized in defect modes of PBG structures.

Acknowledgements. This research was inspired by numerous illuminating discussions with late Professor N.I. Koroteev. This study was supported in part by the Constellation Group GmbH (Austria). A.T. and A.Z. also gratefully acknowledge the support from INTAS project no. 97-0369.

References

1. E. Yablonovitch: *J. Opt. Soc. Am. B* **10**, 283 (1993)
2. J. Joannopoulos, R. Meade, J. Winn: *Photonic Crystals* (Princeton University Press, Princeton 1995)
3. M. Scalora, R.J. Flynn, S.B. Reinhardt, R.L. Fork, M.J. Bloemer, M.D. Tocci, C.M. Bowden, H. Ledbetter, J. Bendickson, J.P. Dowling, R.P. Leavitt: *Phys. Rev. E* **54**, R1078 (1996)
4. N.I. Koroteev, S.A. Magnitskii, A.V. Tarasishin, A.M. Zheltikov: *Opt. Commun.* **159**, 191 (1999)
5. N. Bloembergen, A.J. Sievers: *Appl. Phys. Lett.* **17**, 483 (1970); J. Martorell, R. Vilaseca, R. Corbalan: *Appl. Phys. Lett.* **70**, 702 (1997); M. Scalora, M.J. Bloemer, A.S. Manka, J.P. Dowling, C.M. Bowden, R. Viswanathan, J.W. Haus: *Phys. Rev. A* **56**, 3166 (1997)
6. L.A. Golovan', A.M. Zheltikov, P.K. Kashkarov, N.I. Koroteev, M.G. Lisachenko, A.N. Naumov, D.A. Sidorov-Biryukov, V.Yu. Timoshenko, A.B. Fedotov: *JETP Lett.* **69**, 300 (1999)
7. P.M. Goorjian, A. Taflove: *Opt. Lett.* **17**, 180 (1991); A. Taflove: *Computational Electrodynamics: The Finite-Difference Time-Domain Method* (Artech House, Norwood, MA 1995)
8. P. Tran: *Opt. Lett.* **21**, 1138 (1996)
9. E. Vasilyeva, A. Taflove: *Opt. Lett.* **23**, 1155 (1998)
10. U. Gruening, V. Lehmann, S. Ottow, K. Busch: *Appl. Phys. Lett.* **68**, 747 (1996)
11. J.G. Fleming, S.-Y. Lin: *Opt. Lett.* **24**, 49 (1999)
12. R.D. Meade, K.D. Brommer, A.M. Rappe, J.D. Joannopoulos: *Appl. Phys. Lett.* **61**, 495 (1992)
13. B. Engquist, A. Majda: *Math. Comput.* **31**, 629 (1977)
14. M.A. Paesler, P.J. Moyer: *Near-Field Optics* (Wiley, New York 1996)
15. V. Sandoghdar, S. Wegscheider, G. Krausch, J. Mlynek: *J. Appl. Phys.* **81**, 2499 (1997)
16. M.K. Lewis, P. Wolanin, A. Gafni, D.G. Steel: *Opt. Lett.* **23**, 1111 (1998)
17. S. Hunter, F. Kiamilev, S. Esener, D.A. Parthenopoulos, P.M. Rentzepis: *Appl. Opt.* **29**, 2058 (1990); D.A. Akimov, A.B. Fedotov, N.I. Koroteev, S.A. Magnitskii, A.N. Naumov, D.A. Sidorov-Biryukov, A.M. Zheltikov: *Jpn. J. Appl. Phys.* **36**, Part 1, 1B, 426 (1997)